Ocean Sci. Discuss., 11, 2691–2732, 2014
www.ocean-sci-discuss.net/11/2691/2014/
doi:10.5194/osd-11-2691-2014

Ocean Science
Discussions
Open Access

Modelling of the anthropogenic tritium transient and its decay product helium-3 in the Mediterranean Sea using a high-resolution regional model

M. Ayache[1], **J.-C. Dutay**[1], **P. Jean-Baptiste**[1], **K. Beranger**[2], **T. Arsouze**[2], **J. Beuvier**[3,4], **J. Palmieri**[1], **B. Le-vu**[1], and **W. Roether**[5]

[1]Laboratoire des Sciences du Climat et de l'Environnement (LSCE), IPSL, CEA/UVSQ/CNRS, Orme des Merisiers, Gif-Sur-Yvette, France
[2]ENSTA ParisTech, Palaiseau, France
[3]Mercator-Océan, Ramonville Saint-Agne, France
[4]CNRM-GAME (Météo-France, CNRS), Toulouse, France
[5]Institut für Umweltphysik, Univ. Bremen, Bremen, Germany

Received: 23 October 2014 – Accepted: 18 November 2014 – Published: 5 December 2014

Correspondence to: M. Ayache (mohamed.ayache@lsce.ipsl.fr)

Published by Copernicus Publications on behalf of the European Geosciences Union.

Abstract

This numerical study provides the first simulation of the anthropogenic tritium invasion and its decay product helium-3 (^{3}He) in the Mediterranean Sea. The simulation covers the entire tritium (^{3}H) transient generated by the atmospheric nuclear-weapon tests performed in the 1950s and early 1960s and run till 2011. Tritium, helium-3 and their derived age estimates are particularly suitable for studying intermediate and deep-water ventilation and spreading of water masses at intermediate/deep levels. The simulation is made using a high resolution regional model NEMO-MED12 forced at the surface with prescribed tritium evolution derived from observations.

The simulation is compared to measurements of tritium and helium-3 performed along large-scale transects in the Mediterranean Sea during the last few decades on cruises of Meteor M5/6, M31/1, M44/4, M51/2, M84/3, and Poseidon 234. The results show that the input function used for the tritium, generates a realistic distribution of the main hydrographic features of the Mediterranean Sea circulation. In the eastern basin, the results highlight the weak formation of Adriatic Deep Water in the model, which explains its weak contribution to the Eastern Mediterranean Deep Water in the Ionian sub-basin. It produces a realistic representation of the Eastern Mediterranean Transient signal, simulating a deep-water formation in the Aegean sub-basin at the beginning of the 1993, with a realistic timing of deep-water renewal in the eastern basin. In the western basin, the unusual intense deep convection event of winter 2005 in the Gulf of Lions during the Western Mediterranean Transition is simulated. However the spreading of the recently ventilated deep water toward the South is too weak. The ventilation and spreading of the Levantine Intermediate Water from the eastern basin toward the western basin is simulated with realistic tracer-age distribution compared to observation-based estimates.

1 Introduction

Several recent studies show that the Mediterranean Sea will be particularly sensitive to climate change impacts (Giorgi, 2006; Diffenbaugh and Giorgi, 2012). This basin is surrounded to the north by highly industrialized countries and to the south by countries with high population growth; these factors amplify the existing environmental and water resource problems, and intensify anthropogenic pressure on the basin (Attané and Courbage, 2004; MerMex-Group, 2011).

Although relatively small, the Mediterranean Sea (Fig. 1) is of sufficient size for its circulation to be governed by large-scale ocean dynamics. It is among the most interesting of our planet's semi-enclosed seas because of the great range of processes and interactions which occur within it (Malanotte-Rizzoli and Robinson, 1988): most physical processes which characterize the global general ocean circulation occur directly or analogously in the Mediterranean Sea. All major forcing mechanisms, including air–sea interaction, buoyancy fluxes and lateral mass exchange, are present, as well as intermediate and deep-water masses formation (POEM-group, 1992). It thus makes an excellent laboratory test basin for studying processes that affect the global thermohaline circulation.

The circulation of the Mediterranean Sea is usually described in a schematic way as an open thermohaline cell with two closed secondary cells, one for each sub-basin (Lascaratos et al., 1999). In the principal cell incoming Atlantic Water (AW) is transformed at the surface to the outflowing Levantine Intermediate water (LIW), which is the main contributor of the Mediterranean outflow into the Atlantic (MOW). The two secondary cells describe the development of Western and Eastern Mediterranean Deep Waters (Lascaratos et al., 1999). Deep-water source areas are classically the Adriatic sub-basin for the Eastern Mediterranean Basin (EMed) basin and the Gulf of Lions (Liguro-Provencal sub-basin) for the Western Mediterranean Basin (WMed) (Millot and Taupier-Letage, 2005). The main product of intermediate waters is the LIW (Levantine Intermediate Water) formed in the eastern Levantine sub-basin, at between 200 and

OSD
11, 2691–2732, 2014

500 m depth and spreading out across the entire Mediterranean basin. The Aegean sub-basin is also considered as a source of deep (Cretan Deep Water, CDW) and intermediate waters (Cretan Intermediate Water, CIW) for the EMed. The CIW was found in the layer below the Levantine Intermediate Water (LIW) between about 500 and 1200 m depth (Theocharis et al., 2002; Schlitzer et al., 1991). The out-flowing CDW is no longer dense enough to reach the bottom of the adjacent basins, but ventilates from layers between 1500 and 2500 m (Theocharis et al., 2002). All abbreviations and acronyms used in the paper are given in Table 1 (CIESM, 2001).

Millot (2013) suggests that the correct name for the intermediate waters outflowing from the eastern basin should not be LIW, but should be the Eastern Intermediate Water (EIW) considered as an evolution of the CIW and LIW (and the tEMDW, after the Eastern Mediterranean Transient, EMT, event) peaks combined together rather than an evolution of the LIW peak alone. The overall formation rate of intermediate and deep MWs is estimated to be 90 % of the AW inflow at Gibraltar (10 % being evaporated), of which 3/4 and 1/4 are formed in the Eastern and Western basin, respectively. These values lead to an average residence time of 50–100 years (Millot and Taupier-Letage, 2005).

The circulation of the various waters from/to Gibraltar to/from the zones of deep convective sinking is reasonably well-understood, although finer scale structures are still debated. The formation of the deep waters is also characterized by a decadal variability. The two most recent examples being the EMT (Roether et al., 2007), and the Western Mediterranean Transient (WMT) (Schroeder et al., 2008). The EMT is a period, at the beginning of the 1990s, during which the main deep-water formation site in the EMed was switched from the Adriatic sub-basin to the Aegean sub-basin. The WMT started during the mid-2000s (winter 2005) in the Gulf of Lions, during which a huge volume of WMDW was formed with unusually high temperature and salinity. These two events give a good illustration of the impact of decadal variability in the Mediterranean Sea and have been confirmed by observation. However, as the observations are discrete

OSD
11, 2691–2732, 2014

in time and space, they have not led to quantification and a complete understanding of these events.

The large-scale circulation patterns and the deep-water ventilation are difficult to measure directly. Various concepts of our present knowledge of ocean ventilation were originally deduced from the distributions of hydrographic tracers such as salinity, oxygen, and nutrients (Broecker and Peng, 1982). Hydrographic tracers, however, tell us little about the time rates of the processes that are involved in ocean ventilation (Doney, 1992). With the development of in situ measurement techniques, oceanographers have increasingly turned to transient tracer species, in particular radiocarbon, tritium, and the chlorofluorocarbons (Broecker and Peng, 1982). These geochemical tracers provide additional information that allows us to constrain time scale of ocean ventilation. In this paper, we use tritium (^{3}H) and its decay product helium-3 (^{3}He) to evaluate the circulation simulated by a high resolution model of the Mediterranean Sea.

An ocean general circulation model is an excellent tool for investigating the mechanisms that control the present ocean circulation, such as the inter-basin exchange of the thermohaline circulation (Beranger et al., 2004; Gasparini et al., 2005), and allows us to assess different hypotheses proposed to explain exceptional events. It also provides an opportunity for investigating the future evolution of the Mediterranean Sea circulation and its effect on the climate of that region (Drobinski et al., 2012; Beuvier et al., 2010; Herrmann et al., 2010; Somot et al., 2006). However, these increasingly used models should be validated to test their realism against in situ observations. Passive tracers such as anthropogenic tritium and helium-3 are particularly suitable for evaluating the large scale dynamics simulated by these models on decadal time scales.

The present study provides the first simulation of the tritium/helium-3 distribution, and its age-related tracer distribution, using a high-resolution regional model of the entire Mediterranean Sea. The simulations run between 1950 and 2011, which cover the period of nuclear bomb tests in the atmosphere in the late 1950s and early 1960s. Simulated tritium/helium-3 concentrations in the water column are compared with observations from Meteor cruises: M5/6-1987; M31/1-1995; M44/4-1999; M51/2-2001;

M84/3-2011, and Poseidon 232-1997. These data allows us to critically examine the dynamics of the ocean general circulation model NEMO-MED12 (Lebeaupin Brossier et al., 2011; Beuvier et al., 2012; Palmieri et al., 2014) and to evaluate the ability of this model to reproduce the main features of the circulation and mixing of the Mediterranean Sea water masses and their interannual variability, including the exceptional events observed in the ventilation of the deep waters.

2 Presentation of tracers

Tritium was almost the first transient tracer to be used extensively in oceanography (see, e.g., Östlund, 1969; Clarke et al., 1976). It is a powerful tracer for studying thermocline ventilation as well as chlorofluorocarbons (Sarmiento and Gruber, 2006). Tritium is the only radioactive isotope of hydrogen that decays by beta emission to ^{3}He, the stable isotope of helium with a half-life of 12.32 years (Lucas and Unterweger, 2000). It is produced in the upper atmosphere by cosmic ray spallation and fast neutron interactions with ^{14}N to form one ^{3}H atom and ^{12}C, and after oxidation to tritiated water (HTO), it takes part in the hydrological cycle. The anthropogenic tritium (mainly from atmospheric nuclear weapon tests) was added to the atmosphere in significant amounts in the 1950s and early 1960s. This completely masked the natural background of tritium (Weiss et al., 1979). The input of tritiated water from the atmosphere to the ocean involves several factors, such as precipitation, evaporation, and runoff (Weiss et al., 1979). The tritium signal that entered the surface of the ocean provides an interesting tracer of ocean circulation on time-scales from a few years up to a few decades (Jenkins, 1987). Tritium is reported in conventional Tritium Units (TU), in which 1 TU is a tritium to hydrogen (^{3}H / H) ratio of 10^{-18}.

Tritium ratio in the Mediterranean surface waters rose to 25–30 TU in 1964, a factor of about 100 above the natural level (Fig. 2), and thereafter declined 30-fold up to 2011(Roether et al., 2013). This decline was due to a combination of its radioactive decay (half-life of 12.32), which produced significant quantities of helium-3, and mixing

OSD
11, 2691–2732, 2014

with the deeper water masses (Roether et al., 2013). Limitations in the use of tritium alone, as a water mass tracer, arise from its radioactive nature and from dispersion of the bomb signal in the ocean, leading to difficulties in interpreting the tritium distribution. These limitations can be partially overcome by using tritium in combination with its decay product helium-3. This isotope is a useful tracer for investigating the deep ocean circulation and for evaluating ocean general circulation models, because it is a stable and conservative nuclide that does not take part in any chemical or biological processes. Helium-3 is a rare isotope of helium, found essentially in solubility equilibrium with its atmospheric concentration at the surface, with a slightly lower $^{3}He/^{4}He$ ratio in sea water than in the atmosphere ($\delta He_{sw} = -1.8\,\%$, where ($\delta He_{sw}(\%) = 100(R_{sw}/R_{air} - 1)$ where $R = {}^{3}He/^{4}He$ and $R_{air} = 1.384 \times 10^{-6}$) (Clarke et al., 1976; Farley et al., 1995). Helium-3 in the ocean originates from three different sources: namely, (i) gas dissolution in equilibrium with atmospheric helium, (ii) addition by radioactive decay of tritium (called tritiugenic helium-3), and (iii) by injection of helium-3 into the oceans by the hydrothermal activity at deep sea spreading ridges, and also from the sediment above crusts by α-decay of heavy elements (called terrigenic helium-3). The most commonly used method of isolating the tritiugenic portion of helium-3 is the two-step procedure of Roether et al. (1998, 2001), using concurrent values of He, $\delta^{3}He$ and neon (Ne) concentration, because the Ne generates a similar excess as the ^{3}He, but has no sources in the ocean interior. This methodology has already been applied on tritium data by Roether et al. (1998, 2013).

Jenkins and Clarke (1976) combined measurements of ^{3}H and ^{3}He to estimate the elapsed time since the water parcel has been isolated from exchange with the atmosphere, when the ^{3}H-^{3}He clock is set to zero (called the ^{3}H-^{3}He age). This method has been employed in various fields in addition to oceanography (e.g., Jenkins, 1982, 1987).

Discussion Paper | Discussion Paper | Discussion Paper | Discussion Paper |
OSD
11, 2691–2732, 2014
Modelling of the anthropogenic tritium transient
M. Ayache et al.

The ^{3}H-^{3}He age is set for an isolated parcel of water that does not contain an excess of helium-3 at the initial time at the surface. It is, defined as:

$$^3\mathrm{H}_{(t)} = {}^3\mathrm{H}_0 \cdot \mathrm{e}^{-\lambda t} \quad (1)$$

$$^3\mathrm{He}_{(t)} = {}^3\mathrm{H}_0 \left(1 - \mathrm{e}^{-\lambda t}\right) \quad (2)$$

$$\tau = \lambda^{-1} \cdot \ln\left(\left([^3\mathrm{H}] + \left([^3\mathrm{He}]\right) / [^3\mathrm{H}]\right)\right) \quad (3)$$

where τ in years is the ^{3}H-^{3}He age, $^3\mathrm{H}_0$ is the initial concentration of ^{3}H, λ is the decay constant = $(\ln 2)/T_{1/2}$, when $T_{1/2}$ is the half-life for ^{3}H.

This age, τ, combines the information implicit in the two tracers, while at the same time largely eliminating the dependence on initial conditions. Ages derived from tracers are not conserved during mixing (Jenkins and Clarke, 1976). Mixing tends to reduce the value of the age tracer compared to the real age. This was quantified by Jenkins (1987) in terms of an advection–diffusion relationship for the ^{3}H-^{3}He age. He showed that for areas away from the turbulent boundary regions, such the subtropical gyre, the ^{3}H-^{3}He age is accurate to within 10 % for time-scales less than a decade, and for time-scales of a few decades, the bias is of order 20–30 %. Moreover, in frontal regions and where mixing is more important, the interpretation is more complex. Even though Eq. (3) is non-linear, its use offers many advantages in analyzing tracer data, because the boundary condition for the age is well known at the surface, which reduces the uncertainty associated with the tracer input function.

3 Method

3.1 Description of the model

The model used in this work is a free surface ocean general circulation model NEMO (Madec and the NEMO Team, 2008) in a regional configuration called NEMO-MED12 (Beuvier et al., 2012a). NEMO-MED12 covers the whole Mediterranean Sea and also extends into the Atlantic Ocean to 11° W (buffer zone). The horizontal resolution of the NEMO-MED12 grid is 1/12°, thus varying in latitude between 6.5 and 8 km from 46° N to 30° N, and between 5.5 and 7.5 km in longitude. This scale permits representation of mesoscale features (see a comparison with the first Rossby deformation radius in the Mediterranean Sea in Beuvier et al., 2012a). The vertical resolution (50 levels) ranges from 1 m in the upper layer, to 450 m at bottom. We use partial-steps to adjust the last numerical level with the bathymetry. NEMO-MED12 is the result of a suite of Mediterranean regional versions of OPA and NEMO: OPAMED16 (Beranger et al., 2005), OPA-MED8 (Somot et al., 2006), NEMO-MED8 (Beuvier et al., 2010). NEMO-MED12 has been used to study the anthropogenic carbon uptake (Palmieri et al., 2014), the mixed layer response under high-resolution air–sea forcings (Lebeaupin Brossier et al., 2011), the WMDW formation (Beuvier et al., 2012a), and the transport through the Strait of Gibraltar (Soto-Navarro et al., 2014). Full details of the model and its parameterizations are given by Beuvier et al. (2012a) and Palmieri et al. (2014).

The initial conditions (temperature, salinity) for the Mediterranean Sea, come from the MedAtlas-II (MEDAR/MedAtlas-group, 2002; Rixen et al., 2005) climatology weighted by a low-pass filter with a time window of ten years using the MedAtlas data covering the 1955–1965 period following Beuvier et al. (2012b). The simulation then starts with the initial conditions of an ocean at rest, close to the state of the Mediterranean Sea in October 1958. For the Atlantic buffer zone, the initial state comes from the 2005 World Ocean Atlas for temperature (Locarnini et al., 2006), and salinity (Antonov et al., 2006). River runoff is taken from the interannual dataset of Ludwig et al. (2009) and Vörösmarty et al. (1996). The Black Sea is not included in NEMO-MED12, but input from the Black Sea is considered as runoff using the estimates of Stanev and Peneva (2002).

This simulation was forced by the atmospheric fluxes from the high-resolution (50 km) ARPERA dataset (Herrmann and Somot, 2008; Herrmann et al., 2010). NEMO-MED12 is forced by ARPERA daily fields of the momentum, evaporation and heat fluxes over the period 1958–2013. For the sea-surface temperature (SST) a relaxation term is

OSD
11, 2691–2732, 2014

applied for the heat flux (Beuvier et al., 2012a). The exchanges with the Atlantic Ocean are performed through a buffer zone between 11° W and the Strait of Gibraltar, where 3-D temperature and salinity model fields are relaxed to the observed climatology (Beuvier et al., 2012b). To conserve the Mediterranean Sea's water volume, the total sea-surface height (SSH) is restored in the Atlantic buffer zone from the GLORYS1 reanalysis (Ferry et al., 2010). A 1.5 turbulent closure scheme (Turbulent Kinetic Energy, TKE) is used for the vertical eddy diffusivity (Blanke and Delecluse, 1993) with an enhancement of the vertical diffusivity coefficient (see Beuvier et al., 2012a).

The atmospheric forcing used by Beuvier et al. (2012a) includes some modifications to improve dense water fluxes through the Cretan Arc during the EMT. Beuvier et al. (2010) showed that the previous version of NEMO-MED at 1/8° resolution (NEMO-MED8) was able to reproduce a transient in deep water formation as observed for the EMT, but the simulated transient produced less EMDW. In order to improve simulation of the EMT event, the ARPERA forcing over the Aegean Sea is modified by increasing mean winds and heat loss. More specifically, during the winters of 1991–1992 and 1992–1993, daily water loss is increased by 1.5 $mm\,d^{-1}$, surface heat loss is increased by 40 $W\,m^{-2}$, and the daily wind stress modulus by 0.02 $N\,m^{-2}$. This results in mean wintertime increases in water loss (+41 %), heat loss (+18 %) and wind intensity (+17 %) over the Aegean sub-basin (for more details see Beuvier et al., 2012b; Palmieri et al., 2014).

The simulations are performed "off-line" using pre-calculated dynamical fields derived from (Beuvier et al., 2012a, b), in order to reduce computational costs. The same approach was used by Palmieri et al. (2014) in simulations using CFC and anthropogenic CO_2 as passive tracers. This choice is justified by the fact that these tracers are passive. Their injection does not alter the dynamics of the ocean, and they have no influence on the physical properties of water, unlike the hydrographic tracers such as temperature or salinity.

OSD
11, 2691–2732, 2014

3.2 Tracer boundary conditions

The usefulness of anthropocentric ^3H as a tracer of oceanic processes is strongly limited by our knowledge of the tritium boundary condition at the air–sea interface. Generally, there are two methods of determining the boundary conditions for oceanic tritium simulations. The first method consists of prescribing the temporal evolution of the tritium concentration over the entire surface of the ocean from the available observations (Jia and Richards, 1996). This method can be applied only in those basins where the observations are sufficient to accurately constrain the tritium concentration in surface water (such as the North Atlantic, and the Mediterranean Sea). The second method is to calculate the net flux of tritium from the atmosphere to the ocean, as a function of the hydrological variables (precipitation, evaporation, relative humidity, and river runoff), available in climatological databases (Sarmiento, 1983).

Levels of tritium in precipitation are relatively well-documented, the data are held centrally by the Global Network of Isotopes in Precipitation (GNIP) of the International Atomic Energy Agency and the World Meteorological Organization (Doney et al., 1992). Mathematical formulations have been developed from the GNIP measurement network to represent the spatio-temporal variations of tritium concentrations with rainfall, such as the formulation of Weiss and Roether (1980), and Doney et al. (1992). The tritium levels in water vapour are much less well-documented compared to those in precipitation, which has prevented appropriate formulations being developed. Determinations of tritium content in water vapour are generally based on the content of tritiated water (^3H_2O) in precipitation. Weiss and Roether (1980) assumed tritium equilibrium (ratio about 0.85) between precipitation and marine water vapour. This approach represents a significant source of uncertainty in the input function, and it is difficult to verify this hypothesis because of the transient nature of the tritium in the water vapour. The levels of tritium in rivers are also very poorly documented. However, except for the Adriatic subbasin, rivers make a small contribution to the Mediterranean Sea (Weiss and Roether, 1980).

OSD
11, 2691–2732, 2014

For this study, we used two time series of the tritium concentration in the Mediterranean surface waters (between 1950 and 2011, Fig. 2) developed for the eastern basin by Roether et al., (2013), and for the western basin the curve is homothetic to that of the east, with ratios constrained by available tritium surface data of: *Odysseus*-1965 (Ostlund, 1969); *Phycemed*-1981 (Andrié and Merlivat, 1988); *Origny*-1972, *Poseidon* 232-1997 and *Meteor* 84-2011 (Roether et al., 2013); and *Dewex*-2013 (S. Charmasson, personal communication, 2014). In the Mediterranean Sea the tritium concentrations at the surface are relatively high compared to the global ocean, because of the intra-continental situation of the basin. Indeed, levels of tritium on the continent are generally higher compared to those in the oceans, because on land, rainwater re-evaporates without significant dilution. Note that the EMed surface-water tritium concentrations have always exceeded those in the WMed due to reduced influence of the Atlantic, for which the tritium surface water concentrations have generally been lower (Dreisigacker and Roether, 1978).

In our simulations, we, therefore, used the first method, as we directly prescribe the tritium concentrations for each basin with a transition zone between the two basins created by a linear interpolation of these two time series in the Strait of Sicily. In addition to prescribing the surface tritium concentrations (for each year), we impose a zero concentration of tritiugenic helium-3 (produced only by the radioactive decay of tritium) in the surface layer. Over time, the radioactive decay of tritium produces helium-3, following the law of radioactive decay, which generates the concentration of the tritiugenic helium-3 in the water column. In this study, we simulate only the tritiugenic helium-3 (anthropocentric source), without representing the terrigenic helium-3 component (natural source). To isolate this tritiugenic helium-3 component in the observations, we apply the procedure of Roether et al. (1998, 2001).

OSD
11, 2691–2732, 2014

4 Results

4.1 Global distributions

We begin our analysis by providing a descriptive overview of the global horizontal distribution of the two modelled tracers (tritium and helium-3), and of the derived tracer age. We average between depths of 380 and 540 m, as representative of the intermediate waters, including the LIW layer, and between 1000 and 1600 m depths (below the permanent thermocline) for the deep waters. Figures 3–6 present the model results for 1987, 1995, 1999 and 2011, respectively. These horizontal maps show the distributions of tracers, for the intermediate waters in upper (maps a, c and e), and below for deep water (maps b, d and f). The analysis at these two levels provides a good visualization of the source of ventilation for the interior of the Mediterranean Sea, and the connection between the surface, intermediate and deep water.

The tracer distributions in 1987 (pre-EMT) display a classical situation for the Mediterranean Sea circulation. Relatively high tritium concentrations are simulated in the intermediate waters over whole the EMed, except in the northern Levantine basin considered as the main source of LIW, and south of France in the Gulf of Lions where the source of WMDWs is located. Consequently the tritium penetration is more important in these regions, where higher tritium concentrations are simulated in the deep waters compared to the surrounding waters. The lowest helium-3 concentrations in intermediate waters of EMed are located in the south of the Adriatic sub-basin (Fig. 3c) as a result of subsurface mixing caused by significant intermediate water formation. The tracer age distribution in 1987 (Fig. 3e and f) highlights the region with recent water mass ventilation. It shows a good consistency between the youngest water, with tracer age under 7 years, and the area characterized by low levels of ^{3}He and with a high ^{3}H concentration, especially in the Levantine sub-basin, off the south of France, and the Adriatic sub-basin.

In 1995 gradients throughout the Mediterranean become more pronounced for the spatial tritium distribution in both intermediate and deep waters. The contrast is

OSD
11, 2691–2732, 2014

particularly pronounced in the deep waters between the Ionian and the Levantine sub-basin. The same evolution is observed in the Gulf of Lions (in the western basin), with tritium levels being relatively uniform in the deep water. The evolution of the spatial distribution of helium-3 is complementary and related to the penetration of tritium (Fig. 4c and d). The lower concentrations (between 1.5 and 5 %) marked in the Aegean sub-basin, are mostly due to vertical ocean mixing in this region, and an input of surface water depleted in helium-3. The outflow of water through the Straits of the Cretan Arc related with the EMT is characterized with a deep penetration of water enriched with tritium, and depleted in helium-3 (Fig. 4d), which has been uniquely strengthened during the EMT event occurring in the early 1990s (EMT, Roether et al., 1996, 2007).

The tracer ages calculated in March 1995 confirm the origin of the formation of the deep water and provide an additional estimate for the duration of the mechanism of ventilation. The model produces significant ventilation around the Cretan Arc, illustrated by the very young ages (under 5 years) that are a result of the abrupt change in the EMed during the EMT. That event generates massive penetration of dense water rich in tritium and depleted in helium-3 in the deep Aegean sub-basin. The EMT also causes a remarkable rejuvenation over the Levantine sub-basin with ^{3}H-^{3}He age under 10 years. Outside of this region, water is becoming older, with a maximum of 25 years at Gibraltar.

Parallel to Figs. 3 and 4, Fig. 5 presents the results in 2005. The tracer distribution in the eastern basin has again become more similar to the classical helium-3 distribution observed in 1987. The tritium distribution between the intermediate and deep waters is similar, but is more uniform in the deep water. The maximum tritium concentration in the deep water near the Cretan Arc (Fig. 5b) has disappeared when compared to the situation in 1995. The helium-3 distribution also varies rather little across the deep water in the EMed (Fig. 5d). The main difference simulated in 1995 is a reversal of the areas of intense deep convection between the eastern and western basin. The reduction of the vertical mixing around the Cretan Arc after the EMT generates an increase of helium-3 concentration in the deep water in this region (9 % in 2005 compared to

5 % in 1995). On the other hand, a significant amplification of mixing in the WMed especially in the Gulf of Lions (displayed in Fig. 5d) is characterized by the presence of water very depleted in helium-3 (about 7 %) in the deep waters.

The ^{3}H-^{3}He age distribution in 2005 (Fig. 5e and f) confirms the deep convection event being unusually intense in the Gulf of Lions during winter 2004–2005 (Beuvier et al., 2012a). This event is clearly visualized south of France, with the spread of relatively young deep-water masses (15 years compared to the surrounding water that exceeds 25 years). In the eastern basin, and unlike in 1995, the tracer age is higher south of the Cretan Arc (almost double compared to 1995), and the minimum age for the intermediate waters is more pronounced in the Adriatic sub-basin returning towards the pre-EMT situation.

The tracer distribution in 2011 (Fig. 6) is similar to 1987 when no anomalous rate of deep-water formation occurs. The age is increasing in the deep waters of the two basins. After the EMT event, the Aegean Deep Water (AeDW) is less dense, and cannot penetrate at great depths, leaving space for the older Adriatic Deep Water (AdDW). Similarly in the western basin after the WMT event, the waters become increasingly older, with ages reaching 35 years in the Algerian sub-basin.

4.2 Model evaluation against in situ data

In the following we evaluate and analyze the simulated temporal evolution of tritium and helium-3 in the Mediterranean Sea against in situ observations from Meteor (cruises M5/6-1987; M31/1-1995; M44/4-1999; M51/2-2001; M84/3-2011), and *Poseidon* 234-1997.

The left column of Fig. 7 (Maps a, b, c, d and e) represents the evolution of the tritium distribution in the eastern basin between 1987 and 2011. In 1987 (Fig. 7a), observations are characterized by relatively high tritium concentration (> 3.6 TU) in the upper water masses (< 500 m depth) for all the section except the Levantine sub-basin before passing Crete at 28° E, where the maximum has a lower value in this LIW source area. The tritium concentration decreases rapidly with depth, marking a significant vertical

OSD
11, 2691–2732, 2014

gradient. The model correctly produces the tritium concentration in the first 500 m of the water column, with maximum values of tritium (more than 4.4 TU) in agreement with observations. Deeper, the performance is more contrasted. In the eastern part of the section the model overestimates the penetration of tritium into the intermediate waters. It also tends to underestimate the tritium penetration in the deep Ionian sub-basin, where it fails to produce the maximum concentration associated with EMDW formation (Fig. 7a).

In 1995 (Fig. 7b) we observed, in both model and observation, a reduction of tritium concentration in the surface layer as a result of mixing with the deeper water masses more depleted in tritium, and the ventilation of LIW, and also as a result of radioactive tritium decay. In 1995 we observed an important penetration of tritium into the deep waters near the Cretan Arc as a consequence of the EMT that enriched bottom tritium concentration giving it a value close to the surface value. The model correctly produces the evolution of the tritium distribution between the dilution in the surface layer, and the downward penetration of these tritium rich waters to great depths (about 2400 m depth) between 22 and 26° E (Fig. 7b). However, there is still a disagreement between model and observations in the western part of this section, since the AdDW signal was not sufficiently ventilated before EMT (see Fig. 7a). The penetration of tritium at the bottom is progressing throughout the basin between 1995 and 2001, especially with the propagation of the signal of recent ventilation from the Cretan Arc (Fig. 7c). The dilution of the tritium concentration in the sub-surface water is still correctly simulated between 1999 and 2001. However, at the bottom the model still underestimates the tritium concentration at the two borders east and west of these sections, as for the previous years. In 2011 the tritium concentration is reduced throughout the basin due to mixing and radioactive decay.

The same sections presented for tritium, were also performed for helium-3, which allows us to investigate in more detail the LIW ventilation. Along the transect performed in 1987 (Fig. 7f), surface values are close to the solubility equilibrium of ^{3}He, and the maximum of ^{3}He clearly marked the LIW layer between 330 and 600 m depth. The

OSD
11, 2691–2732, 2014

lowest values are observed near to the LIW source areas, and the highest towards the two ends of this section with a maximum value near the Strait of Sicily (about 11 %, see Fig. 7f) associated with the higher tritium concentrations observed there. Further down there is a strong decrease of ^{3}He concentration for all the section, with a maximum concentration associated with EMDW in the Ionian basin. The model currently reproduces the maximum of helium-3 concentration in the intermediate waters, with values similar to observations, except in the eastern part of the section where it tends to be overestimated. Deeper, we again clearly note the shortfall associated with the too weak EMDW formation in the Adriatic sub-basin, with too low simulated helium-3 values.

In 1995, the helium-3 maximum is still clearly seen in the LIW layer, but a significant reduction is observed near the Cretan Arc with a value between 4 and 5 %. An important penetration of ^{3}He is observed in deep water at 26° E (Fig. 7g) following the amplification of the ocean mixing by the EMT. The model correctly reproduces this evolution of the helium-3 distribution during this event. In 1999 the concentration in LIW layer is more uniform in both model and in situ observation, the deep maximum associated with EMT ventilation is less pronounced compared to the 1995 situation.

Comparison with the observed helium-3 (after correction for terrigenic ^{3}He) suggests a good agreement between simulated helium-3 and data for the LIW layer, but too high values in the east. As already analyzed for tritium, the model underestimates the helium-3 signal associated with AdDW formation. On the other hand the model has correctly simulated the deep-water formation during the EMT event.

The right column of Fig. 7, presents the tracer age estimation, along the sections in the eastern basin. In 1987, the first 500 m of the surface layer had a low age, characterized by a high tritium concentration across all the EMed except near the LIW formation area (between 28 and 30° E) where the mixing with older deep waters depleted in tritium increases the tracer age in this region. Deeper, the ^{3}H-^{3}He age increases gradually with a maximum at the two borders of the section, respectively in the Levantine and Ionian sub-basins (near the Strait of Sicily).

OSD
11, 2691–2732, 2014

In 1995, the minimum age layer is shallower, the values are lower in the centre of the section between 26 and 28° E, with the outflow of waters from the Cretan Arc, which brings young waters (10 years) up to 2400 m depth in the Levantine sub-basin. Old waters are observed at the bottom in the eastern part of the section (32° E), the maximum age before the Strait of Sicily is even more pronounced compared to 1987.

The waters become generally older all over the section in 1999. The youngest waters are still located in the centre of the EMed and the maximum age at the western end. In addition to that we have a significant evolution of the tracer age distribution in the deep waters in the Eastern Levantine basin. Younger water propagation at the bottom generates a transfer of the oldest water between 1000 and 1500 m depth (26–34° E). In 2001 the water column structure is very similar to the situation in 1999 with a progressive propagation of old water from the two borders of the EMed. In 2011, the age of the water masses has increased in the whole eastern basin, but still with pronounced maxima at depths between 1000 and 2000 m near the two ends of the section.

The model correctly simulates the observed evolution of the tracer age distribution. It does particularly well at reproducing the evolution associated with the amplification of deep-water formation around the Cretan Arc during the EMT. The propagation of younger water into the bottom of the Levantine sub-basin creating a maximum age at between 1000 and 2000 m depth, simulated at a realistic time scale by the model. The deep-water accumulation before the Strait of Sicily is also successfully simulated with tracer-age close to that estimated from observation.

The results in the WMed (the Alboran, Algerian and Tyrrhenian sub-basins), together with observations made during the *Poseidon* 234 and *Meteor* 84/3 cruises in 1997 and 2011, respectively (presented by circles in our sections) are shown in Fig. 8. The observations on the section made from *Poseidon* (1997) show a steady decline of ^{3}H concentration from 2 TU at the surface to a minimum of 0.6 TU near 2000 m depth. In particular, lower tritium concentration is observed in the Tyrrhenian sub-basin, a basin with no deep-water formation and where WMDW mixes with the intermediate water outflows (mainly the LIW and CIW) from the Strait of Sicily. In 2011 (Fig. 8b) the tritium gradient was basically the same as in 1997, but with a lower value in the intermediate water, with concentration decreasing from 0.85 TU at the surface to 0.2 TU at 2000 m depth. In the bottom of the Algerian sub-basin a relatively higher value of tritium concentration is observed, compared to the Alboran sub-basin.

In 1997 the maximum value of helium-3 is centred near 500 m depth, a layer occupied by the LIW (Fig. 8c). Above the LIW, the values decrease gradually into the surface layer, which has a helium-3 concentration in equilibrium with the atmosphere. Below the LIW, the decrease of helium-3 is more moderate, leading to 9.5 % near to 2000 m. In 2011 the helium-3 maximum is more shallow (appears between 700 and 1500 m) with a higher concentration over the entire water column. The lower values of helium-3 in the bottom of the Algerian sub-basin (10 % compared to 12 % in the surrounding waters) are related to the WMDW ventilation signal. The ^3H-^3He age distributions highlights differences in deep-water mass ventilation along these sections (Fig. 8). In 1997 the intermediate waters have basically the same tracer age, but in the deep waters the lower ages are noticeable in the Algerian sub-basin at 6° E, with the maximum in the Tyrrhenian sub-basin. In 2011 the age distribution presents similar gradients, but with older ages throughout the entire water column.

The particularly intense deep convection event of winter 2005 gives the largest volume of dense water formed compared to the 1997 situation, with this pronounced penetration water rich in helium-3 occupied the whole water column. The spreading of WMDW formed in winter 2005 southwards into the Algerian sub-basin was detected with a noticeable signature in helium-3 concentration, where a minimum is observed at the bottom of the southern part of the Algero-Provencal sub-basin.

The model correctly simulates the main features of the tracer distributions and their evolution with time between the two cruises (Fig. 8). The pronounced LIW signal in helium-3 in 1997 is particularly well-simulated as well as its penetration in depth with time. The contrast in deep-water mass ventilation between these two sub-basins is well-simulated. The model produces older bottom water masses in Tyrrhenian sub-basin, and the signal related to the propagation of deep-water masses formed in the

OSD
11, 2691–2732, 2014

Gulf of Lions is simulated. However, the penetration of new WMDW is weaker in the simulation compared to what was deduced from in situ observations. We simulate the presence of a low helium-3 concentration at the bottom of the Algero-Provencal sub-basin, but this signal is still lower than in situ observations.

5 Discussion

The ^{3}H-^{3}He simulation provides an independent and additional constraint for modelled water masses ventilation. The evolution of mixing in convection areas and spreading of recently ventilated water at intermediate/deep levels was evaluated by comparison with the observations. Several available observations along large-scale sections allowed a careful evaluation of model performance in the Mediterranean Sea on a decadal time scale. The tritium input function based on data from historical tritium time series was tested for the first time in this work. Severe mismatches between model and observations are clearly associated with shortcomings in model physics, otherwise this parameterization led to realistic values of the tracer distribution in the water column. These results suggest that this approach is appropriate for generating a tritium simulation sufficiently valid to evaluate model performance on decadal time scales in the Mediterranean Sea.

The variations of the thermohaline circulation on decadal time scale are well-documented by the available ^{3}H-^{3}He observations. The simulation of these tracers has shown that the main feature of the ventilation and variability of the thermohaline circulation is well-captured by the NEMO-MED12 model. First, the realistic dilution and penetration of the tritium signal from the surface waters indicates that the model generates a realistic mixing with sub-surface water masses over the whole basin. This result indicates that the vertical mixing parameterization used in our model, the TKE closure at order 1.5, is capable of generating a satisfying connection between the surface and sub-surface waters.

Discussion Paper | Discussion Paper | Discussion Paper | Discussion Paper |

OSD
11, 2691–2732, 2014

Modelling of the anthropogenic tritium transient

M. Ayache et al.

The available observations in the eastern basin have allowed us to evaluate and validate the temporal evolution of the main water masses ventilation, simulated by the model between 1987 and 2011.

Before the EMT (represented here by the 1987 situation), the distribution of the tracer is well-structured (Fig. 7a) and reflects a classical distribution of the water masses. The LIW layer is especially characterized by a maximum of helium-3 concentration between 300 and 700 m, and with lower values closest to the LIW formation area east of Rhodes island. The model simulates correctly the main features of the formation and ventilation of the LIW, producing a vertical distribution of the tracer in agreement with the observations in the intermediate waters. The model particularly demonstrates realistic performance in the Ionian sub-basin upstream the Strait of Sicily. It produces a strong accumulation of the tracers in the intermediate waters (Fig. 7a and f), that is observed and associated with the presence of the CIW (Cretan Intermediate Water), which joins the LIW (Schlitzer et al., 1991; Roether et al., 1999). Evidence for its presence is provided by the enhanced concentrations of the tracer in the intermediate waters of this area. However, in the eastern part of the Levantine sub-basin, the model tends to overestimate the ventilation of LIW and to generate too high a helium-3 concentration compared to observations. Generation of tritiugenic ^{3}He has now become small relative to the situation in the previous decades (Fig. 2). Therefore the signature of tracers in the LIW layer has decreased significantly between 1987 and 2011. This evolution in the tracer distribution is also noticeable in our simulations. Indeed the tritium distribution in 2011 was far smoother compared to previous years; on the other hand, helium-3 in this year presents a similar distribution compared to those found earlier, but with a gradual decline. This depletion of helium-3 is evidence of a displacement by upwelling that feeds into the westward return flow, to be eventually transferred into the WMed. The model correctly produces the aging of the waters masses observed in 2011.

The LIW represents the principal movement of water mass from the EMed into the WMed. The tracer-age of the Levantine Intermediate Water (LIW) during the spreading from the Levantine sub-basin (LIW source zone), to the Strait of Sicily is estimated in

OSD
11, 2691–2732, 2014

our simulation at between 9 and 12 years, and more than 22 ± 4 years in the WMed before Gibraltar (Fig. 3). These transit times are in good agreement with the observations by Roether et al. (2013), which estimate a transit time of 12 ± 2 years at the entrance into the Strait of Sicily and 22 ± 4 years in the WMed. Our estimation is also comparable with values obtained by Gacic et al. (2013) based on salinity anomalies. Exchange processes between EMed and WMed is a fundamental mechanism for the thermohaline circulation in the Mediterranean Sea. This result demonstrates that the model simulates this mechanism with the same time scale as in situ observations. Moreover, the model then simulates a satisfying propagation of the LIW into the western basin, demonstrated by the realistic lateral propagation of the associated helium-3 maximum signal at intermediate depth and its downward penetration with time between 1997 and 2011 (Fig. 8).

The tracer simulation has also enabled us to evaluate the formation of deep water and its associated temporal and spatial variability, and to study its impact on the deep-water mass renewal over the basin. In the eastern basin, before the EMT (1987, Fig. 7), the signal of deep-water ventilation from the Adriatic sub-basin is too shallow in the simulation compared to observations. This shortcoming was also found in a Chlorofluorocarbon (CFC) simulation with the same model NEMO-MED12 (Palmieri et al., 2014). In the Adriatic sub-basin, the contribution of rivers is very important, however, the atmospheric forcing ARPERA combined with the river runoff dataset overestimate the freshwater flux, and provide too much freshwater on this domain. This result in unusually low salinity water compared to observations, and further prevents winter convection, and therefore the AdDW formed is too light and not dense enough to propagate to the bottom of the Ionian sub-basin.

The sequence of the EMT events occurring in the eastern basin at the beginning of the 1990s has completely changed the deep-water mass structure. The evolution of the tritium distribution between 1995 and 2001 demonstrates that the water mass structure was very different from the pre-EMT picture (see Fig. 7). These sections demonstrate a considerable dilution of tracer concentrations in the surface water, following

OSD
11, 2691–2732, 2014

a significant amplification of mixing in the EMed, when surface water rich in tritium are transferred to the bottom. The model has successfully reproduced this amplification of mixing caused by the EMT and generated an appropriate EMDW ventilation with realistic values of tritium concentration at the bottom. The section in 1995 emphasizes the severe impact of the EMT on water mass distribution, which transfers massive volumes of tritium-rich near-surface waters into the deep layers, with the highest contributions toward the bottom and south of Crete (Fig. 7b), causing a temporary change in the EMDW origin, from the Adriatic to Aegean sub-basin in 1992–1993. Different hypotheses concerning the preconditioning of the EMT and its timing have been proposed in the literature (Malanotte-Rizzoli et al., 1999; Samuel et al., 1999; Josey, 2003). The in situ observations were essential to discover the EMT, but they cannot give a clear description of the ocean evolution between the past and the actual situation, which does not give us a clear choice between the various proposed hypotheses leading to the EMT. On the other hand numerical modelling gives us a clear 4-D description, which provides an additional opportunity to test this different hypothesis proposed by in situ data at larger spatial and temporal scales. Beuvier et al. (2010) have already reproduced the EMT, using a previous configuration of NEMO-MED at $1/8^{\circ}$ degree resolution, but with a weaker formation of dense waters compared to data. The new configuration of NEMO-MED12 at $1/12^{\circ}$ degree resolution, allows a better simulation of the EMT (Beuvier et al., 2011). The outflow of this new very dense water rich in tritium and depleted in helium-3 from the Cretan Arc straits is clearly observed and correctly simulated in 1995 (Fig. 4) compared to the situation in the other years (Figs. 3, 5 and 6), which gives clear evidence that during the EMT, the EMDW was not formed in the Adriatic sub-basin but in the Aegean sub-basin. The ^{3}H-^{3}He age confirms this conclusion considering the pronounced overflow of recently ventilated waters from the Cretan Arc straits in 1995 (Fig. 4e and f) vs. the other years when the EMDW was formed mainly in the Adriatic sub-basin. Among the preconditioning and triggering elements of the EMT suggested in the literature, Beuvier et al. (2010) suggested that the main

OSD
11, 2691–2732, 2014

factors are the intense winter fiuxes over the Aegean sub-basin during winters 1992 and 1993.

The transient evolution of the tracer age, between 1987 and 2001, in the eastern basin clearly shows a renewal of the deep-water masses, and provides an additional diagnostic to assess the time scale of this mechanism. The increased deep convection caused by the EMT, enhanced the propagation of the relatively young waters (recently ventilated) at the bottom of the Levantine sub-basin, which displaced the preceding bottom waters (Fig. 7k) up to 1000 m depth in 2001 (Fig. 7n). The model succeeds in producing this observed renewal of the bottom waters, and reorganization of the deep waters in the eastern basin; the tracer age shows that this mechanism is simulated with a realistic time-scale. The ^{3}H-^{3}He age can hardly be older than the time between the tritium peak and the time of observation. For example the deep waters of the Levantine Sea have a ^{3}H-^{3}He age of no more than about 30 years, while a box-model evaluation (Roether and Schlitzer 1991) gave the true age as about 150 years. The reason is the most pronounced tritium peak in the 1960s, which has the consequence that the pre-peak years have little influence on the age. Only when the bulk of the water leaves the surface at a time when the tritium concentration has decreased sufficiently, does this effect becomes small. In the LIW layer the effect is small because the water is younger and the LIW is largely an advective system, whereas in the deep-waters mixing predominates.

The gradual decline of tritium concentrations in the EMed after 1987 is mainly due to a westward drift of intermediate waters, which renews the waters in the eastern basin, but also due to the cessation of atmospheric nuclear-weapon testing, that reduced the transfer of anthropogenic tritium in the mixed layer, to as little as about twice the natural background level (Roether et al., 2013).

In the western basin the thermohaline circulation cell is driven by deep-water formation in the Gulf of Lions; it spreads from there, with intense mesoscale phenomena along the coastal current. The system of deep convection in the Gulf of Lions had a particularly intense event observed during winter of 2005 (Lopez-Jurado et al., 2005;

Canals et al., 2006; Schroeder et al., 2008) and to a lesser extent during the following years, when the convection occurred over a much larger and deeper area than usual. Winter 2005 was one of the coldest and driest winters in the 40 last years, the strong surface cooling and evaporation with highly favourable preconditioning triggered deep convection. Lopez-Jurado et al. (2005) suggested that the unusual characteristics of the 2005 convection event could be due to a change in characteristics of the water masses advected until the forming zone of WMDWs after EMT. Herrmann et al. (2010) rather suggest that the higher temperature and salinity of the new WMDW formed in 2005 are due to the absence of intense convective winter in the 1990's and early 2000s in the NWMed, leading to an accumulation of heat and salt in the intermediate and deep layers of this area. This intense formation of dense water in the Gulf of Lions has already been simulated by Beuvier et al. (2012a) with the model used in this study. This transition is well represented in our tracer simulation for March 2005 (Fig. 5d), with a pronounced invasion of the helium-3 in the Liguro-Provencal sub-basin.

The Algerian sub-basin (Fig. 8a) presents a relatively higher tritium concentrations and lower values of helium-3 compared to those marked in the Alboran sub-basin, indicating the impact of the newly formed WMDW. However the southern propagation of this recently ventilated water in the deep sea is too slow, as the deep flow is strongly constrained by the interaction between the bathymetry and the eddy activity. In addition, the new WMDW formed in the model is not salty enough with respect to these observations (Beuvier et al., 2012a). Its southwards propagation is also too slow compared to in situ and satellite observations (Beuvier et al., 2012a). The same vertical gradient of tritium observed in 1997 is marked in 2011 in the WMed, but, with lower concentrations in the water column following the drastic reduction of tritium in the atmosphere after the stopping of the atmospheric nuclear-weapon testing. Helium-3 maximum in LIW is deeper (about 1000 m) in 2011, with a significant accumulation of helium-3 in the deep water compared to 1997, which is due to continued tritium decay on the way. This evolution of the tracer signals was successfully reproduced by the model indicating that the conversion of LIW in the western basin is well-simulated.

OSD
11, 2691–2732, 2014

6 Conclusions

The anthropogenic tritium invasion and its decay product helium-3 was simulated for the first time in the Mediterranean Sea, using a high resolution regional model (NEMO-MED12) at 1/12° of horizontal resolution (6–8 km). The formulation used for the tritium boundary conditions led to results of sufficient quality to allow them to be used for evaluating the circulation of the model. Tritium-helium-3 observations available along a number of cruises have allowed us to evaluate the decadal variability of the thermohaline circulation in the Mediterranean Sea. The model correctly simulates the main features of the thermohaline circulation of the Mediterranean Sea, with mechanisms having a realistic time scale compared to estimations from observations. The Eastern Mediterranean Transient (EMT) signal from the Aegean sub-basin was simulated, with its corresponding penetration of tracers into the deep water in early 1995's. The strong convection event of winter 2005 and following years in the Gulf of Lions was also well-reproduced in the simulation. The tracer-age diagnostic provided an interesting tool to assess the ventilation and propagation of intermediate and deep water. We show that some main features of decadal evolution of waters masses are well-simulated by the model. Especially the transient evolution of the tracer age in the eastern basin revealed that the renewal of the bottom waters masses is correctly simulated after the EMT. The connection between the eastern basin towards the western basin, undertaken by the spreading of the Levantine Intermediate Water (LIW) is realistically simulated with transit times (between 17 and 26 years), comparable with other estimates.

However, some aspects in the simulation still need to be improved. In the eastern basin, the tracer simulation results highlight the too weak formation of Adriatic Deep Water (AdDW), followed by a weak contribution to the Eastern Mediterranean Deep Water (EMDW) in the Ionian sub-basin. The production of WMDW is correct but the spreading of the recently ventilated deep water to the South of the western basin is too weak. Also the LIW is well represented by the helium-3 signal, but shows too high

OSD
11, 2691–2732, 2014

values in the eastern end of EMed, due to overestimation of the formation of LIW in this region.

Our work proposes additional constraints on the subsurface circulation and ocean mixing processes in the Mediterranean Sea. These new tracer simulations and their comparison with recent in situ observations and with other tracer elements (like CFC, carbon-14. . . , etc.) provide a new and additional expertise to assess and improve the dynamical regional model NEMO-MED12. This evaluation was fundamental before using NEMO-MED12 as dynamical components in coupled models for studying the evolution of the climate and its effect on the biogeochemical cycles in the Mediterranean Sea, and is essential to improve our ability to predict the future evolution of the Mediterranean Sea under the increasing anthropogenic pressure.

References

Andrié, C. and Merlivat, L.: Tritium in the western Mediterranean Sea during 1981 Phycemec cruise, Deep-Sea Res. Pt. I, 35, 247–267, 1998.

Antonov, J. I., Locarnini, R. A., Boyer, T. P., Mishonov, A. V., and Garcia, H. E.: World Ocean Atlas 2005, Vol. 2 Salinity, edited by: Levitus, S., NOAA Atlas NESDIS 62, US Government Printing Office, Washington, D. C., 182 pp., 2006.

Attané, I. and Courbage, Y.: Demography in the Mediterranean region: situation and projections, Plan Bleu, 2004.

Béranger, K., Mortier, L., Gasparini, G.-P., Gervasio, L., Astraldi, M., and Crépon, M.: The dynamics of the Sicily Strait: a comprehensive study from observations and models, Deep-Sea Res. Pt. II, 51, 411–440, 2004.

Béranger, K., Mortier, L., and Crépon, M.: Seasonal variability of water transport through the Straits of Gibraltar, Sicily and Corsica, derived from a high-resolution model of the Mediterranean circulation, Prog. Oceanogr., 66, 341–364, 2005.

Beuvier, J.: Modélisation de la variabilité climatique et des masses d'eau en mer Méditerranée: Impact des échanges océan-atmosphère, Ph. D. thesis, Ecole Polytechnique, Palaiseau, France, 2011.

OSD
11, 2691–2732, 2014
Modelling of the anthropogenic tritium transient
M. Ayache et al.

Beuvier, J., Sevault, F., Herrmann, M., Kontoyiannis, H., Ludwig, W., Rixen, M., Stanev, E., Béranger, K., and Somot, S.: Modeling the Mediterranean Sea interannual variability over the last 40 years: focus on the EMT, J. Geophys. Res., 115, C08017, doi:10.1029/2009JC005950, 2010.

Beuvier, J., Béranger, K., Lebeaupin Brossier, C., Somot, S., Sevault, F., Drillet, Y., Bourdallé-Badie, R., Ferry, N., and Lyard, F.: Spreading of the Western Mediterranean Deep Water after winter 2005: Time scales and deep cyclone transport, J. Geophys. Res., 117, C07022, doi:10.1029/2011JC007679, 2012a.

Beuvier, J., Lebeaupin Brossier, C., Béranger, K., Arsouze, T., Bourdallé-Badie, R., Deltel, C., Drillet, Y., Drobinski, P., Lyard, F., Ferry, N., Sevault, F., and Somot, S.: MED12, Oceanic component for the modelling of the regional Mediterranean Earth System, Mercator Ocean Q. Newslett., 46, 60–66, 2012b.

Blanke, B. and Delecluse, P.: Low frequency variability of the tropical Atlantic Ocean simulated by a general circulation model with mixed layer physics, J. Phys. Oceanogr., 23, 1363–1388, 1993.

Broecker, W. S. and Peng, T.-H.: Tracers in the Sea: Palisades, NY, Lamont-Doherty Geol. Observ., 1982.

Canals, M., Puig, P., Durrieu de Madron, X., Heussner, S., Palanques, A., and Fabres, J.: Flushing submarine canyons, Nature, 444, 354–357, 2006.

Clarke, W. B., Jenkins, W. J., and Top, Z.: Determination of tritium by mass spectrometric measurement of ^{3}He, Int. J. Appl. Radiat. Isot., 27, 515–522, 1976.

Diffenbaugh, N. S. and Giorgi, F.: Climate change hotspots in the CMIP5 global climate model ensemble, Climatic Change, 114, 813–822, 2012.

Doney, S. C., Glover, D. M., and Jenkins, W.: A model function of the global bomb tritium distribution in precipitation, 1960–1986, J. Geophys. Res, 97, 5481–5492, 1992.

Dreisigacker, E. and Roether, W.: Tritium and 90-strontium in North Atlantic surface water, Earth Planet. Sci. Lett., 38, 301–312, 1978.

Drobinski, P., Anav, A., Lebeaupin Brossier, C., Samson, G., Stéfanon, M., Bastin, S., Baklouti, M., Béranger, K., Beuvier, J., Bourdallé-Badie, R., Coquart, L., D'Andrea, F., de Noblet-Ducoudré, N., Diaz, F., Dutay, J. C., Ethe, C., Foujols, M. A., Khvorostyanov, D., Madec, G., Mancip, M., Masson, S., Menut, L., Palmieri, J., Polcher, J., Turquety, S., Valcke, S., and Viovy, N.: Model of the Regional Coupled Earth system (MORCE): application to process and climate studies in vulnerable regions, Environ. Modell. Softw., 35, 1–18, 2012.

Farley, K. A., Maier-Reimer, E., Schlosser, P., and Broecker, W. S.: Constraints on mantle 3 He fluxes and deep-sea circulation from an oceanic general circulation model, J. Geophys. Res., 100, 3829–3839, 1995.

Ferry, N., Parent, L., Garric, G., Barnier, B., and Jourdain, N. C.: Mercator Global Eddy Permitting Ocean Reanalysis GLORYS1V1: Description and Results, Mercator Ocean Q. Newslett., 36, 15–28, 2010.

Gacic, M., Schroeder, K., Civitarese, G., Cosoli, S., Vetrano, A., and Eusebi Borzelli, G. L.: Salinity in the Sicily Channel corroborates the role of the Adriatic–Ionian Bimodal Oscillating System (BiOS) in shaping the decadal variability of the Mediterranean overturning circulation, Ocean Sci, 9, 83–90, doi:10.5194/os-9-83-2013, 2013.

Gasparini, G.-P., Ortona, A., Budillon, G., Astraldi, E., and Sansone, M.: The effect of Eastern Mediterrranean Transient on the hydrographic characteristics in the Strait of Sicily and in the Tyrrhenian Sea, Deep-Sea Res. Pt. I, 32, 915–935, 2005.

Giorgi, F.: Climate change hot-spots, Geophys. Res. Lett., 33, L08707, doi:10.1029/2006GL025734, 2006.

^{3}H-^{3}He Surveys: Tritium and helium isotopes in the ocean, Columbia University, Earth Institute, available from: https://www.ldeo.columbia.edu/environmental-tracer-group/3h3he-survey (last access: 3 December 2014), 2013.

Herrmann, M. and Somot, S.: Relevance of ERA40 dynamical downscaling for modeling deep convection in the Mediterranean Sea, Geophys. Res. Lett., 35, L04607, doi:10.1029/2007GL032442, 2008.

Herrmann, M., Somot, S., Sevault, F., Estournel, C., and Déqué, M.: Modeling the deep convection in the northwestern Mediterranean Sea using an eddy-permitting and an eddy-resolving model: case study of winter 1986–1987, J. Geophys. Res., 113, C04011, doi:10.1029/2006JC003991, 2008.

Herrmann, M., Sevault, F. Beuvier, J., and Somot, S.: What induced the exceptional 2005 convection event in the northwestern Mediterranean basin? Answers from a modeling study, J. Geophys. Res., 115, C12051, doi:10.1029/2010JC006162, 2010.

Jenkins, W. J.: On the climate of a subtropical ocean gyre: decade timescale variations in water mass renewal in the Sargasso Sea, J. Mar. Res., 40, 265–290, 1982.

Jenkins, W. J.: ^{3}H and ^{3}He in the Beta triangle; observation of gyre ventilation and oxygen utilization rates, J. Phys. Oceanogr., 17, 763–783, 1987.

OSD

11, 2691–2732, 2014

Modelling of the anthropogenic tritium transient

M. Ayache et al.

Jenkins, W. J. and Clarke, W. B.: The distribution of ^{3}He in the western Atlantic Ocean, Deep Sea Res., 23, 481–494, 1976.

Jia, Y. and Richards, K. J.: Tritium distributions in an isopycnic model of the North Atlantic, J. Geophys. Res., 101, 11883–11901, 1996.

Josey, S.: Changes in the heat and freshwater forcing of the eastern Mediterranean and their influence on deep water formation, J. Geophys. Res., 108, C3237, 2003.

Lascaratos, A., Roether, W., Nittis, K., and Klein, B.: Recent changes in deep water formation and spreading in the eastern Mediterranean Sea: a review, Prog. Oceanogr., 91, 97–166, 1999.

Lebeaupin Brossier, C., Béranger, K., Deltel, C., and Drobinski, P.: The Mediterranean response to different space–time resolution atmospheric forcings using perpetual mode sensitivity simulations, Ocean Model., 36, 1–25, doi:10.1016/j.ocemod.2010.10.008, 2011.

Locarnini, R. A., Mishonov, A. V., Antonov, J. I., Boyer, T. P., and Garcia, H. E.: World Ocean Atlas 2005, Volume 1: Temperature, S. Levitus, Ed., NOAA Atlas NESDIS 61, US Government Printing Office, Washington, D. C. 182 pp., 2006.

López-Jurado, J., Gonzalez-Pola, C., and Velez-Belchi, P.: Observation of an abrupt disruption of the long-term warming trend at the Balearic Sea, western Mediterranean Sea, in summer 2005, Geophys. Res. Lett., 32, L24606, doi:10.1029/2005GL024430, 2005.

Lucas, L. L. and Unterweger, M. P.: Comprehensive review and critical evaluation of the half-life of tritium, J. Res. Natl. Inst. Stand. Tech., 105, 541–549, 2000.

Ludwig, W., Dumont, E., Meybeck, M., and Heussner, S.: River discharges of water and nutrients to the Mediterranean and Black Sea: major drivers for ecosystem changes during past and future decades?, Prog. Oceanogr., 80, 199–217, doi:10.1016/j.pocean.2009.02.001, 2009.

Madec, G. and the NEMO Team.: Note du Pôle de modélisation, Institut Pierre-Simon Laplace (IPSL), France, NEMO ocean engine, 27, ISSN N1288-1619, 2008.

Malanotte-Rizzoli, P. and Robinson, A. R.: POEM: physical Oceanography of the Eastern Mediterranean, EOS, Transactions American Geophysical Union, 69, doi:10.1029/88EO00125, 1988.

Malanotte-Rizzoli, P., Manca, B. B., Ribera d'Alcala, M., Theocharis, A., Brenner, S., Budillon, G., and Ozsoy, E.: The Eastern Mediterranean in the 80s and in the 90s: the big transition in the intermediate and deep circulations, Dynam. Atmos. Oceans, 29, 365–395, 1999.

MEDAR Group.: Medar-Medatlas Protocol (Version 3) Part I: Exchange Format and Quality Checks for Observed Profiles; P. Rap. Int. IFREMER/TMSI/IDM/SIS002-006, p. 50, 2002.
MERMEX group: Marine Ecosystems Responses to climatic and anthropogenic forcings in the Mediterranean, Prog. Oceanogr., 91, 97–166, 2011.
Millot, C.: Levantine Intermediate water characteristics: an astounding general misunderstanding!, Sci. Mar., 77, 217–232, 2013.
Millot, C. and Taupier-Letage, I.: Circulation in the Mediterranean Sea, The Handbook of Environmental Chemistry, 5, 29–66, doi:10.1007/b107143, 2005.
Östlund, H. G.: Expedition Odysseus.: Tritium and Radiocarbon in the Mediterranean and Black Seas. Report ML 69167, Inst. of Marine and Atmosph. Sciences, Univ. of Miami, 1969.
Palmiéri, J., Orr, J. C., Dutay, J.-C., Béranger, K., Schneider, A., Beuvier, J., and Somot, S.: Simulated anthropogenic CO_2 uptake and acidification of the Mediterranean Sea, Biogeosciences Discuss., 11, 6461–6517, doi:10.5194/bgd-11-6461-2014, 2014.
POEM Group: General circulation of the eastern Mediterranean, Earth Sci. Rev., 32, 285–309, 1992.
Rixen, M., Beckers, J. M., Levitus, S., Antonov, J., and others.: The Western Mediterranean deep water: a proxy for climate change, Geophys. Res. Lett., 32, L12608, doi:10.1029/2005GL022702, 2005.
Roether, W. and Schlitzer, R.: Eastern Mediterranean deep water renewal on the basis of chlorofluoromethane and tritium data, Dynam. Atmos. Oceans 15, 333–354, 1991.
Roether, W. and Well, R.: Oxygen consumption in the Eastern Mediterranean, Deep-Sea Res. Pt. I, 48, 1535–1551, 2001.
Roether, W., Manca, B. B., Klein, B., Bregant, D., Georgopoulos, D., Beitzel, V., Kovacevic, V., and Luchetta, A.: Recent changes in eastern Mediterranean deep waters, Science, 271, 333–335, 1996.
Roether, W., Well, R., Putzka, A., and Ruth, C.: Component separation of oceanic helium, J. Geophys. Res., 103, 27931–27946, 1998.
Roether, W., Beitzel, V., Sultenfuß, J., and Putzka, A.: The Eastern Mediterranean tritium distribution in 1987, J. Mar. Syst., 20, 49–61, 1999.
Roether, W., Klein, B., Manca, B. B., Theocharis, A., and Kioroglou, S.: Transient eastern Mediterranean deep waters in response to the massive dense-water output of the Aegean Sea in the 1990s, Prog. Oceanogr., 74, 540–571, doi:10.1016/j.pocean.2007.03.001, 2007.

OSD
11, 2691–2732, 2014

Modelling of the anthropogenic tritium transient

M. Ayache et al.

Roether, W., Jean-Baptiste, P., Fourré, E., and Sültenfuß, J.: The transient distributions of nuclear weapon-generated tritium and its decay product ^{3}He in the Mediterranean Sea, 1952–2011, and their oceanographic potential, Ocean Sci., 9, 837–854, doi:10.5194/os-9-837-2013, 2013.

Samuel, S., Haines, K., Josey, S., and Myers, P. G.: Response of the Mediterranean Sea thermohaline circulation to observed changes in the winter wind stress field in the period 1980–1993, J. Geophys. Res., 104, 7771–7784, 1999.

Sarmiento, J. L.: A simulation of bomb tritium entry into the Atlantic Ocean, J. Phys. Oceanogr., 13, 1924–1939, 1983.

Sarmiento, J. L. and Gruber, N.: Ocean Biogeochemical Dynamics, Princeton University Press, Princeton, NJ, 526 pp., 2006.

Schlitzer, R., Roether, W., Oster, H., Junghans, H.-G., Hausmann, M., Johannsen, H., and Michelato, A.: Chlorofluoromethane and oxygen in the eastern Mediterranean, Deep-Sea Res. Pt. I, 38, 1531–1551, doi:10.1016/0198-0149(91)90088-W, 1991.

Schroeder, K., Ribotti, A., Borghini, M., Sorgente, R., Perilli, A., and Gasparini, G. P.: An extensive western Mediterranean deep water renewal between 2004 and 2006, Geophys. Res. Lett., 35, L18605, doi:10.1029/2008GL035146, 2008.

Somot, S., Sevault, F., and Déqué, M.: Transient climate change scenario simulation of the Mediterranean Sea for the 21st century using a high-resolution ocean circulation model, Clim. Dynam., 27, 851–879, doi:10.1007/s00382-006-0167-z, 2006.

Soto-Navarro, J., Somot, S., Sevault, F., Beuvier, J., Béranger, K., Criado-Aldeanueva, F., and García-Lafuente, J.: Evaluation of regional ocean circulation models for the Mediterranean Sea at the strait of Gibraltar: volume transport and thermohaline properties of the outflow, Clim. Dynam., 1–16, doi:10.1007/s00382-014-2179-4, 2014.

Stanev, E. V. and Peneva, E. L.: Regional sea level response to global climatic change: Black Sea examples, Global Planet. Change, 32, 33–47, 2002.

Theocharis, A., Klein, B., Nittis, K., and Roether, W.: Evolution and status of the Eastern Mediterranean Transient (1997–1999), J. Mar. Syst., 33–34, 91–116, 2002.

Vörösmarty, C. J., Fekete, B. M., and Tucker, B. A.: Global River Discharge Database (RivDIS V1.0), International Hydrological Program, Global Hydrological Archive and Analysis Systems, UNESCO, Paris, 1996.

Weiss, W. and Roether, W.: The rates of tritium input to the world oceans, Earth Planet. Sci. Lett., 49, 435–446, 1980.

OSD
11, 2691–2732, 2014

Weiss, W., Bullacher, J., and Roether, W.: Evidence of pulsed discharges of tritium from nuclear energy installations in central European precipitation, in: Behaviour of Tritium in the Environment, 17–30, IAEA-SM-232/18, IAEA, Vienna, 1979.
Workshop CIESM Monograph no. 38 on Dynamics of Mediterranean deep waters, edited by: Briand, F., Monaco, 2001.

OSD
11, 2691–2732, 2014

Modelling of the anthropogenic tritium transient

M. Ayache et al.

Table 1. List of acronyms used in the paper.

Acronyms	Meaning
AW	Atlantic Water (Surface water of Atlantic origin)
LIW	Levantine Intermediate Water.
WMDW	Western Mediterranean Deep Water.
TDW	Tyrrhenian Deep Water.
CIW	Cretan Intermediate Water.
NAdDW or NADDW	North Adriatic Deep Water (Formerly NADW).
AdDW	Adriatic Deep Water (Formed in the southern Adriatic, main component of the EMDW and sometimes called SADW).
CDW	Cretan Deep Water
LDW	Levantine Deep Water (Formed in NW Levantine Basin).
EMDW	Eastern Mediterranean Deep Water (Kept for historical reasons).
EOW	Eastern Mediterranean Overflow Water (Sometimes called AIW or tEMDW at the Strait of Sicily).
MOW	Mediterranean Outflow Water (At the Strait of Gibraltar) (MW in the Atlantic).
tEMDW	transitional Eastern Mediterranean Deep Water
EMT	Eastern Mediterranean Transient
WMT	Western Mediterranean Transition
EMed	Eastern Mediterranean Basin
WMed	Western Mediterranean Basin
NWMed	North Western Mediterranean

OSD
11, 2691–2732, 2014

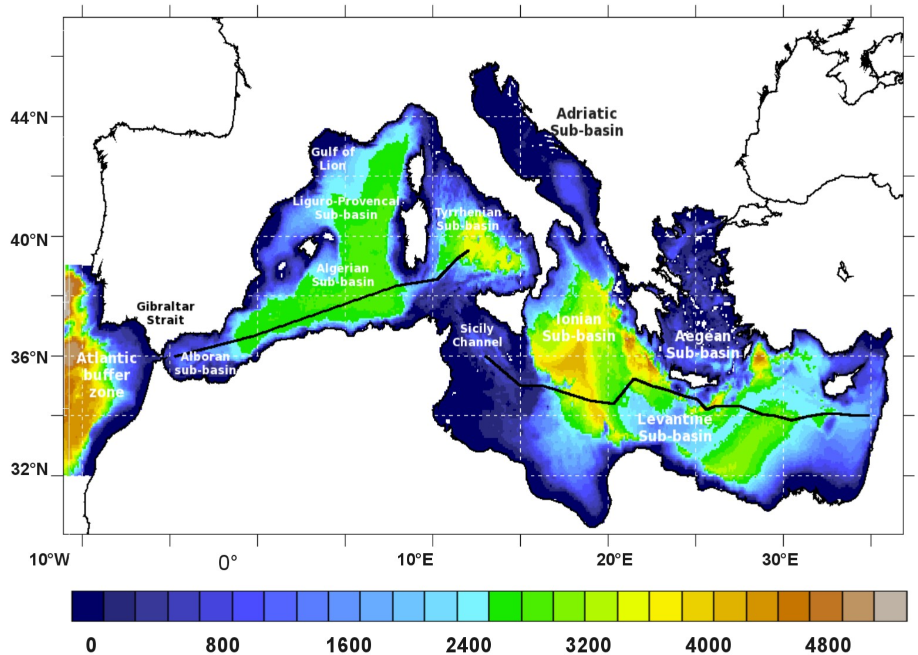

Figure 1. Map of the NEMO-MED12 model domain and bathymetry with location of the main Mediterranean sub-basins. The trans-Mediterranean section from the *Meteor* cruise in 1987, 1995, 1999, 2001 and 2011 for the eastern basin (used in Fig. 7). And of *Poseidon* 234, 1997 Meteor, 84/3, 2011 for the western basin (used in Fig. 8).

OSD
11, 2691–2732, 2014

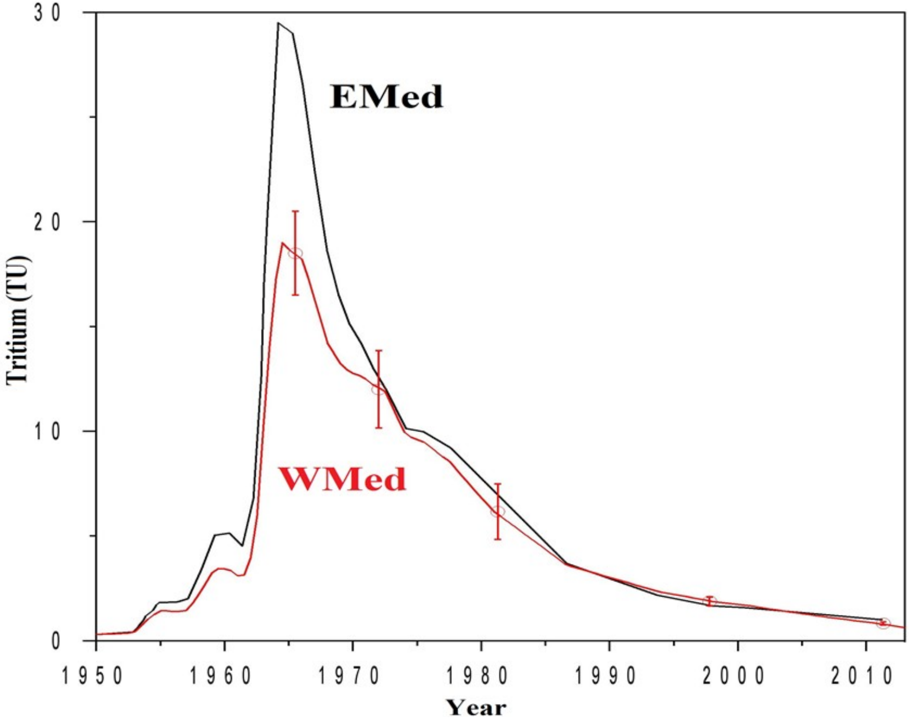

Figure 2. History of tritium concentrations in Mediterranean surface waters. The curve for the eastern basin (in black) is taken from Roether et al. (2013). For the western basin (in red), the curve is homothetic of that of the eastern basin, with ratios constrained by available tritium surface data: ODYSSEUS-1965 (Ostlund, 1969); PHYCEMED-1981 (Andrié and Merlivat, 1988); ORIGNY-1972, POSEIDON232-1997 and METEOR 84-2011 (Roether et al., 2013); DEWEX-2013 (S. Charmasson, personal communication, 2014).

OSD
11, 2691–2732, 2014

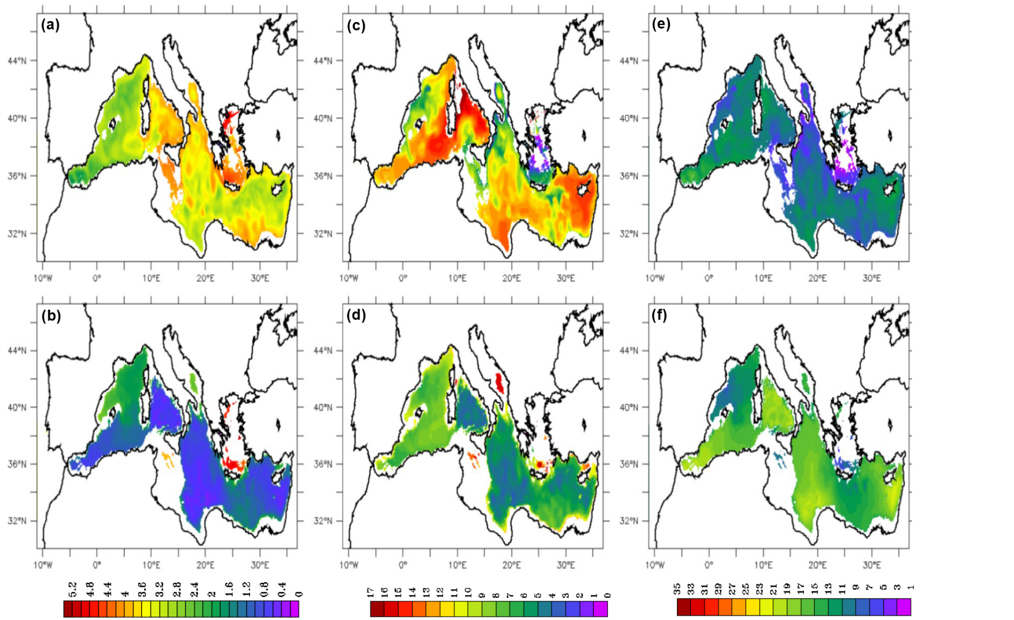

Figure 3. Output of model for March 1987, **(a)** and **(b)** concentrations of tritium (in TU) successively of LIW layer (Average depth between 380 and 540 m) and for the depth layer (average depth between 1000 and 1600 m), **(c)** and **(d)** same for helium-3 (in %), **(e)** and **(f)** idem for the ^{3}H-^{3}He age (in years).

OSD

11, 2691–2732, 2014

Title Page
Abstract | Introduction
Conclusions | References
Tables | Figures
◀| |▶
◀ ▶
Back | Close
Full Screen / Esc
Printer-friendly Version
Interactive Discussion

OSD

11, 2691–2732, 2014

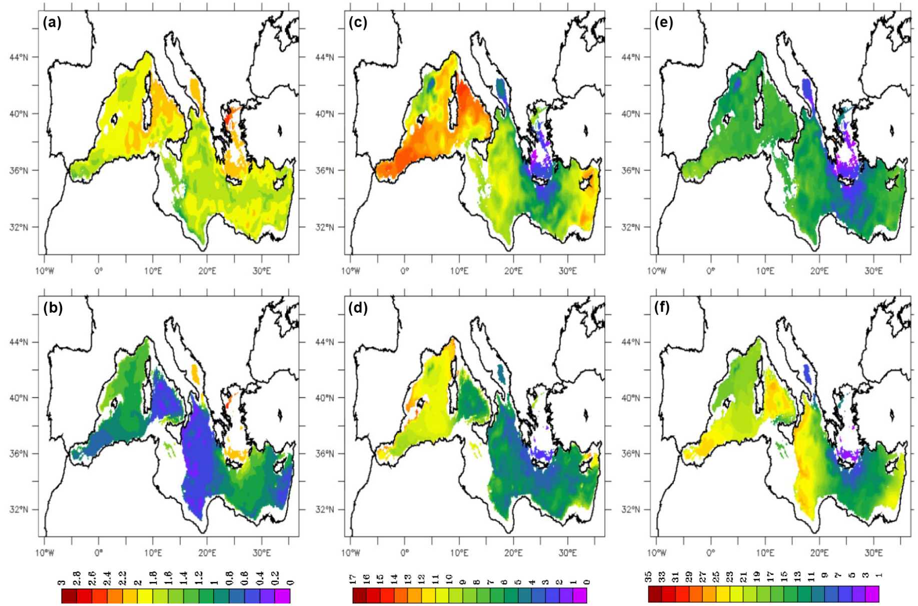

Figure 4. Output of model for March 1995, **(a)** and **(b)** concentrations of tritium (in TU) successively of LIW layer (average depth between 380 and 540 m) and for the depth layer (average depth between 1000 and 1600 m), **(c)** and **(d)** same for helium-3 (in %), **(e)** and **(f)** idem for the ^{3}H-^{3}He age (in years).

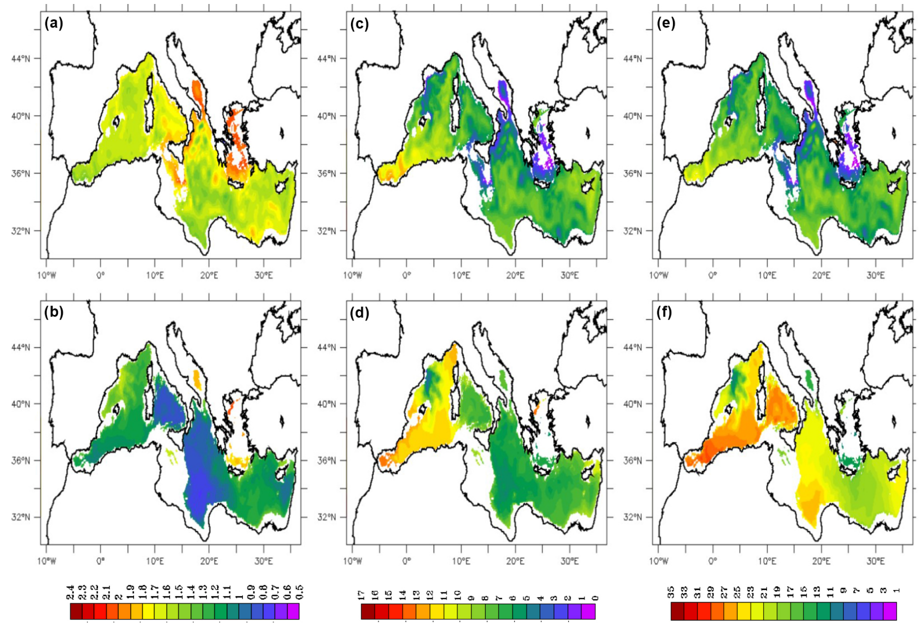

Figure 5. Output of model for March 2005, **(a)** and **(b)** concentrations of tritium (in TU) successively of LIW layer (average depth between 380 and 540 m) and for the depth layer (average depth between 1000 and 1600 m), **(c)** and **(d)** same for helium-3 (in %), **(e)** and **(f)** idem for the ^{3}H-^{3}He age (in years).

OSD
11, 2691–2732, 2014

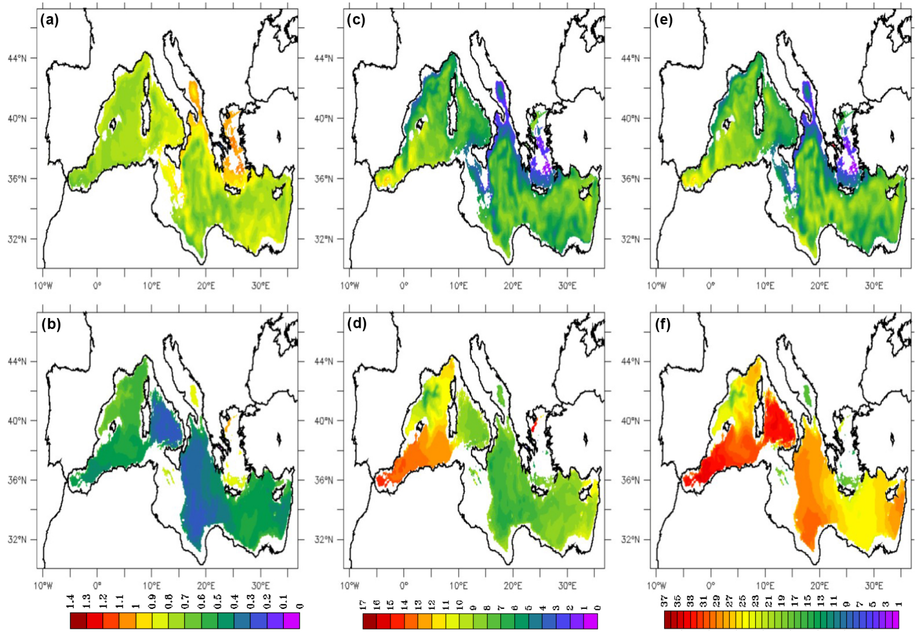

Figure 6. Output of for March 2011, **(a)** and **(b)** concentrations of tritium (in TU) successively of LIW layer (average depth between 380 and 540 m) and for the depth layer (average depth between 1000 and 1600 m), **(c)** and **(d)** same for helium-3 (in %), **(e)** and **(f)** idem for the ^{3}H-^{3}He age (in years).

OSD
11, 2691–2732, 2014

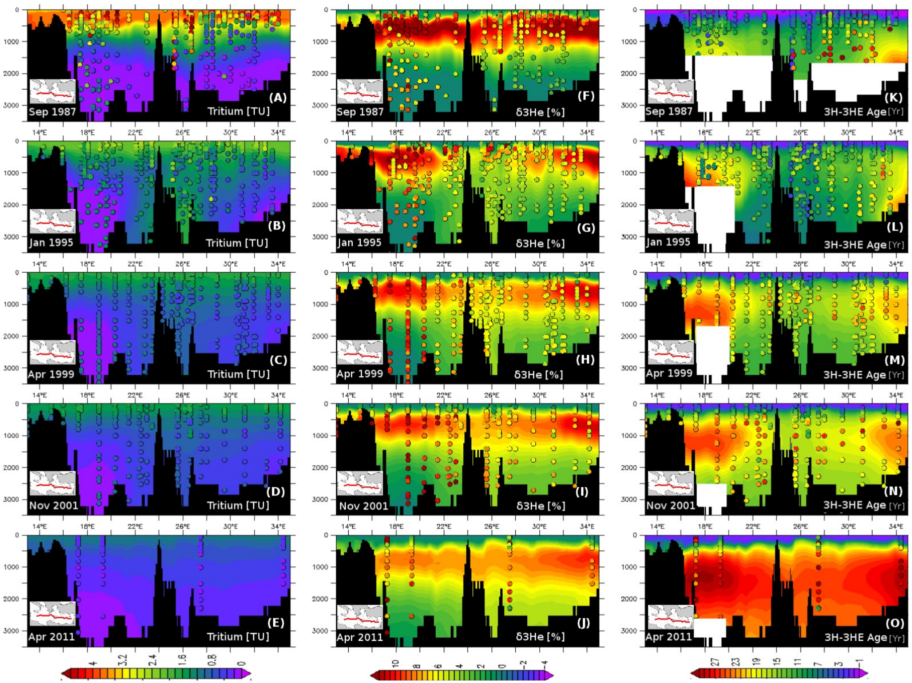

Figure 7. Model data comparison sections in the EMed, in 1987, 1995, 1999, 2001 and 2011. The left column shows tritium concentration in TU, helium-3 in the middle, and the racer age (in years) are shown in the right column. In our simulation we do not calculate the age tracers for the tritium concentration below detection limit (i.e tritium concentration < 0.1 TU). Superimposed circles are the data from Roether et al., 2013.

OSD

11, 2691–2732, 2014

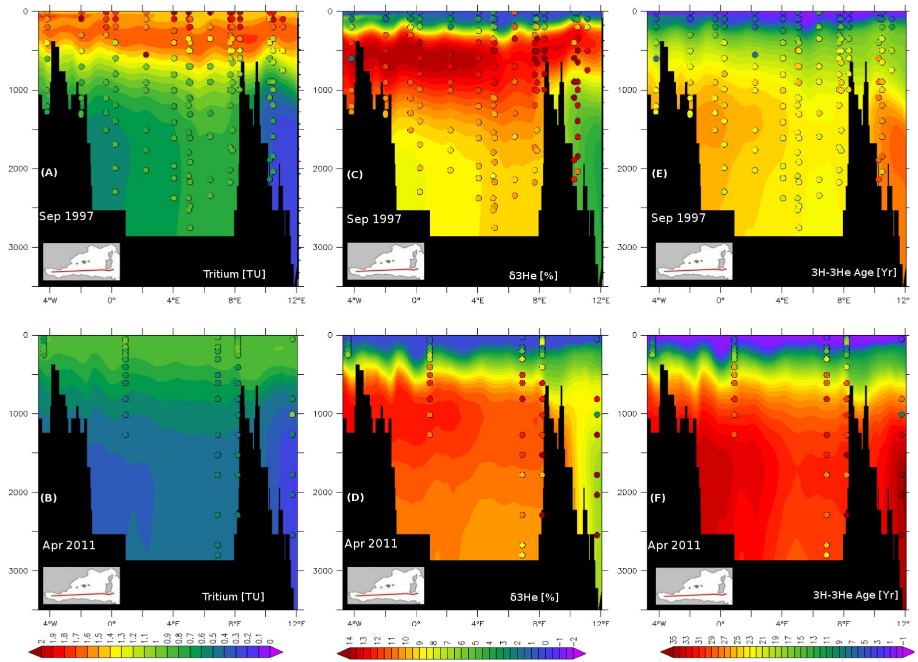

Figure 8. Model data comparison sections in the WMed, in 1997 and 2011. The left column shows tritium concentration in TU, helium-3 in the middle, and the racer age (in years) are shown in the right column. In our simulation we do not calculate the age tracers for the tritium concentration below detection limit (i.e tritium concentration < 0.1 TU). Accompanied with observations made during the cruises of *Poseidon* 234, and *Meteor* 84/3, in 1997 and 2011, respectively.

OSD

11, 2691–2732, 2014

Modelling of the anthropogenic tritium transient

M. Ayache et al.